A model for lignin alteration—part I: a kinetic reaction-network model

D.F. Payne*, P.J. Ortoleva

Laboratory for Computational Geodynamics, Indiana University, Bloomington, IN 47405, USA

Abstract

A new quantitative model is presented which simulates the maturation of lignin-derived sedimentary organic matter under geologic conditions. In this model, compositionally specific reactants evolve to specific intermediate and mobile products through balanced, *n*th order processes, by way of a network of sequential and parallel reactions. The chemical kinetic approach is based primarily on published observed structural transformations of naturally matured, lignin-derived, sedimentary organic matter. Assuming that Upper Cretaceous Williams Fork coal in the Piceance Basin is primarily lignin-derived, the model is calibrated for the Multi-Well Experiment(MWX) Site in this basin. This kind of approach may be applied to other selectively preserved chemical components of sedimentary organic matter. © 2001 Elsevier Science Ltd. All rights reserved.

Keywords: Lignin; Structural transformation; Reaction network; Kinetic; Piceance Basin

1. Introduction

This paper presents a chemical kinetics model of the transformation of lignin-derived sedimentary organic matter under natural sub-surface conditions. The purpose of this model is to simulate a suite of reactions that account for the observed structural transformations using geologically relevant kinetics. At the heart of the model is the understanding of specific bond breaking and cross-linking processes, which are universal to the transformation of sedimentary organic molecules that occur during maturation.

The relative abundance of lignin and its relative resistance to microbial degradation during early diagenesis indicate that it can be selectively preserved and concentrated in some sedimentary deposits (Tegelaar et al., 1989). Thus, it is a large component of many coals, Type III kerogens, and other hydrocarbon precursors.

A significant body of analytical work integrating NMR and pyrolysis analyses has allowed characterization of a representative lignin-derived macromolecular structure and chemistry at various stages of transformation, both in the laboratory and natural settings (Suuberg et al., 1985; Grant and Pugmire, 1989; Solum et al., 1989; Hatcher, 1990; Solomon et al., 1990; Hatcher et al., 1992; Levine, 1993; del Rio et al., 1994; Behar and Hatcher, 1995; Charpenay et al., 1996; Manion et al., 1996; Obeng and Stock, 1996). This model attempts to capture those structural transformations that are inferred from structural and chemical observations, but does not differentiate between microbially-mediated and abiological reactions. Many of the inferred reactions would likely require catalysts to proceed in the geological environment, and microbes are a potential source of catalysts. In addition, it is possible that significant microbial activity on lignin-derived matter could alter the reaction pathways by affecting the early structural transformations. However, this model does not intend to address these issues specifically.

The approach to this model is based on the idea that for a representative lignin-derived macromolecule there are generally a limited number of fundamental substituent

* Corresponding author at current address: US Geological Survey, Peachtree Business Center, Siute 130, 3039 Amwiler Rd., Atlanta GA 30360, USA. Tel.: +1-770-903-9140; fax: +1-770-903-9199.

E-mail address: dfpayne@usgs.gov (D.F. Payne).

groups and linkages, and thus a limited number of processes or reactions that will occur during transformation in the sub-surface environment. Because the kinetics of these processes are intrinsic to the molecular structures (and not the specific molecule) limited kinetic data are required to describe a complicated network of reactions. Ideally, each structural transformation would be modeled in terms of its elementary processes using appropriate reaction rates. In some cases, specific transformations of the lignin-derived macromolecule have been studied by examining the mechanisms of reactions of representative compounds, for example β-O-4 cleavage of guaiacyl (Buchanan et al, 1997). For other transformations, the mechanisms have not been addressed specifically. In such cases, similar representative reactions for which mechanisms and rates are well understood could be used to describe observed transformations, for example decarboxylation (Bell and Palmer, 1994). For transformations involving more speculative mechanisms such as those involving cross-linking, determining appropriate reaction kinetics would be difficult. Bond dissociation energies are probably inappropriate for these reaction activation energies as they represent homolytic cleavage processes, which require higher temperatures than generally exist in sedimentary basins. Because of the uncertainties and inconsistencies in determining reaction mechanisms and rates for elementary processes in the structural transformation of lignin-derived matter, the reactions are composite processes and the kinetics are based on estimates of geological conditions under which the processes occur.

The model is constructed as follows: lignin-derived sedimentary organic matter is defined as a representative initial lignin-derived macromolecule; each transformation of a functional group or molecular structure is described as a single process (many of the transformations require that the representative reaction is non-first order); then, a relative sequence of reaction rates is determined based on the observed relative sequence of the timing of functional group transformations; finally, the reaction rates are calibrated against observed molecular structures and elemental chemistry for samples of independently determined thermal history.

In this paper, we first present a simplified lignin-derived macromolecular structure based on the most commonly observed structural features of fresh and degraded lignin. Observations of the transformations that occur during thermal maturation are discussed in relation to the adopted lignin-derived molecular structure and are described in terms of reactions. The general mathematical formulations to solve the concentrations of species through time are presented. The reaction network is constructed based on observed correlations of structural changes with increasing coal rank, and the kinetics are calibrated for the Multi-Well Experiment (MWX) site in the Piceance Basin in western Colorado.

2. Review of lignin alteration and representative structural transformations

The types of reactions, their relative rates, and their sequence are determined by the observed structural transformations that occur to the lignin-derived molecular structure with increasing maturity up to the high volatile bituminous rank (Hatcher, 1990; Hatcher et al., 1992; del Rio et al., 1994). At higher maturity, observed and inferred transformations in pyrolysis experiments determine the types and relative rates of reaction occurring later in the reaction network (Suuberg et al., 1985; Grant and Pugmire, 1989; Solum et al., 1989; Solomon et al., 1990; Hatcher et al., 1992; Levine, 1993; Behar and Hatcher, 1995; Charpenay et al., 1996; Manion et al., 1996; Obeng and Stock, 1996).

The general processes observed with increasing maturation of lignin-derived molecular structure are: cleavage of the main polymer linkage; modification and loss of various functional groups including methyl, carboxyl, and hydroxyl groups; and cross-linking. Some of the major expected mobile products liberated in the course of structural transformation are methane, carbon dioxide, and water. In order to describe the transformations observed to occur to the lignin-derived macromolecule structure, thirteen types of reactions have been formulated, divided into four classes: isomerization; modification of the propyl structure; defunctionalization; and cross-linking (Table 1).

2.1. Starting material: lignin-derived macromolecular structure

The model requires a relatively unaltered starting material with a defined molecular structure and composition. The lignin-derived macromolecular structure adopted here (Fig. 1) has been modified from Hatcher (1990) to include only the most basic features for the purpose of simplifying of the reaction network. It is a polymer of guaiacyl units linked by the most common types of linkage in lignin, the β-O-4 linkage as well as the α-O-4 linkage with an average of one aryl-methoxyl group per aromatic ring (Fig. 1). According to Hatcher's structure, most of the γ-carbons of the propyl side chains have a hydroxyl substituent. Also, most of the propyl α-carbons that are not part of ether linkages have hydroxyl or carbonyl substituent groups. The model is based on the progressive decomposition of these guaiacyl units into a host of intermediate and mobile species by a network of sequential and parallel reactions.

2.2. Class I: isomerization

The isomerization reaction class comprises the β-O-4 cleavage, which is nearly completed by the time lignin-bearing material has matured to the brown coal rank,

Table 1
Summary of types of reactions accounted for in the model and calibrated activation energy values

Description	General thermal rank of transformation	Figure number	Reaction number	Calibrated activation energy
Class I: isomerization				
β-0-4 cleavage	Peat-brown coal	2a	I	153
Class II: modification of propyl structure				
Oxidation of α-carbonyl to carboxyl	Brown coal–lignite	2b	IIa1, IIa2	163
Oxidation of γ-OH to aldehyde	Uncertain	2c	IIb	161
Oxidation of γ-aldehyde to carboxyl	Uncertain	2c	IIc1, IIc2	163
Reduction of γ-OH to methyl	Peat–lignite	2c	IId	160
Class III: defunctionalization				
Demethoxylation	Peat–sub-bituminous	2d	IIIa1, IIIa2, IIIa3, IIIa4	163
Decarboxylation	Lignite–high volatile bituminous	2e	IIIb1, IIIb2	165
Dehydration	Lignite–sub-bituminous	2f	IIIc1, IIIc2	167, 172
Demethylation of pendant aryl-ethyl	Sub-bituminous–low volatile bituminous	2g	IIId	173
Demethylation of pendant aryl-methyl	Sub-bituminous–low volatile bituminous	2g	IIIe	205
Class IV: cross-linking				
Dehydration and formation of ether linkage	High volatile bituminous–low volatile bituminous	2h	IVa	166
Demethylation	High volatile bituminous–low volatile bituminous	2i	IVb	199
Loss of hydrogen	High volatile bituminous–low volatile bituminous	2j	IVc1, IVc2	213, 216
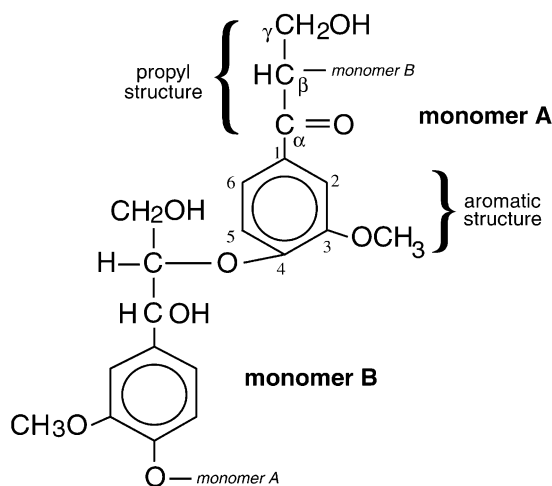
Fig. 1. Simplified model of initial lignin-derived macromolecule structure used in this study; one molecular unit of lignin comprises one monomer each of A and B, except as noted in the lignin composition sensitivity tests.

and results in the creation of a phenol group and the reattachment of the propyl structure to the C3 of the aromatic functional group (Hatcher, 1990) (Fig. 2a). The mechanism of this transformation is still open to debate— whether it is purely a free radical chain mechanism as addressed in thermolytic cleavage experiments (Gilbert and Gajewski, 1982; Britt et al., 1995; Hartgers et al., 1995; Kuroda, 1995) or whether under geologic conditions catalysts such as clays are required for the reaction to occur (Buchanan et al., 1997). As the reaction is nearly complete by the brown coal rank, purely thermolytic reactions probably cannot describe the geologic processes. The choice of mechanism will ultimately have bearing on the way the reaction is modeled in terms of the reaction order and the requirement of other components as reactants or catalysts.

2.3. Class II: modification of the propyl structure

Modification of the propyl structure includes oxidation of the propyl-α alcohol functional group (on monomer B) to a carbonyl functional group, and a subsequent oxidation at that site (on both monomers) to form a carboxyl functional group (Fig. 2b). Progressive oxidation of hydroxylated alkyl side chain carbons is observed in a natural series, eventually leading to decarboxylation: carbonyl functional groups increase as the brown coal rank is approached, and decrease steadily thereafter; carboxyl functional groups increase as the lignite rank is approached, then decrease dramatically between the lignite and the sub-bituminous stages (Hatcher, 1990; del Rio et al., 1994). The carboxyl functional groups are believed to be decreasing from decarboxylation reactions. However, the total CO_2 is more accurately balanced if it has been

sourced by both the carboxyl and carbonyl functional groups (Behar and Hatcher, 1995). Thus, a reaction that transforms carbonyl groups into carboxyl groups is invoked. Although a specific mechanism is not documented, an analogy is made to the anhydride hydrolysis reaction in which anhydride reacts with water to form carbon dioxide by way of a dicarboxyl acid (Petit, 1991; Song et al., 1994). Indeed, water has been suggested as a reactant in the production of CO_2 in pyrolytic experiments (Stalker et al., 1994). Perhaps these reactions can be seen as the progressive oxidation of a hydroxylated alkyl site first to a carbonyl functional group, then to a carboxyl functional group, followed by decarboxylation. Although not specific to the lignin-derived molecular structure, evidence for this may also be seen in the generation of excess CO_2 related to the relative oxidation of asphaltenes during hydrous pyrolysis (Michels et al., 1996). Pyrolysis-methylation data suggest that a likely, though not exclusive location for the formation of ketones and carboxyl functional groups is the α-carbon (del Rio et al., 1994).

The modifications at the propyl γ-site include reduction of the alcohol to a methyl group, oxidation of the alcohol to an aldehyde group, and transformation of the aldehyde to a carboxyl group (Fig. 2c). On the alkyl structure, reduction is suggested to occur as thermal maturity approaches the lignite rank because an increase in carboxyl functional groups is accompanied by a lack of change in total alkyl carbon–oxygen bonds (Hatcher, 1990). In terms of the model's residual macromolecular structure, for every oxygen atom gained in transformation of a carbonyl to a carboxyl group, an oxygen atom must be lost by alkyl dehydration. The oxidation reactions at the γ-site also are not specifically indicated by the structural data, but there is uncertainty in the structural transformations of this site as well as in the location of the aliphatic carbonyl and carboxyl functional groups, so it is possible these reactions occur at this site. As these reactions are written in this paper, the electron transfer processes can be considered as occurring within the molecular structure, and do not require external sources or sinks for electrons, which is an important consideration in non-aqueous reactions, where contact with electron sources or sinks may be limited.

2.4. Class III: defunctionalization

Defunctionalization class reactions include demethoxylation of the aromatic methoxyl functionality, decarboxylation, loss of OH groups on the aromatic structures, and, at higher temperatures, loss of methyl groups attached to the aromatic structure. The loss of the aromatic methoxyl functionality is indicated by NMR data which show that between the unaltered lignin and brown coal rank of a natural series of coalified wood, aromatic methoxyls decrease by about 50%, and by another 50% through the lignite rank, until essentially
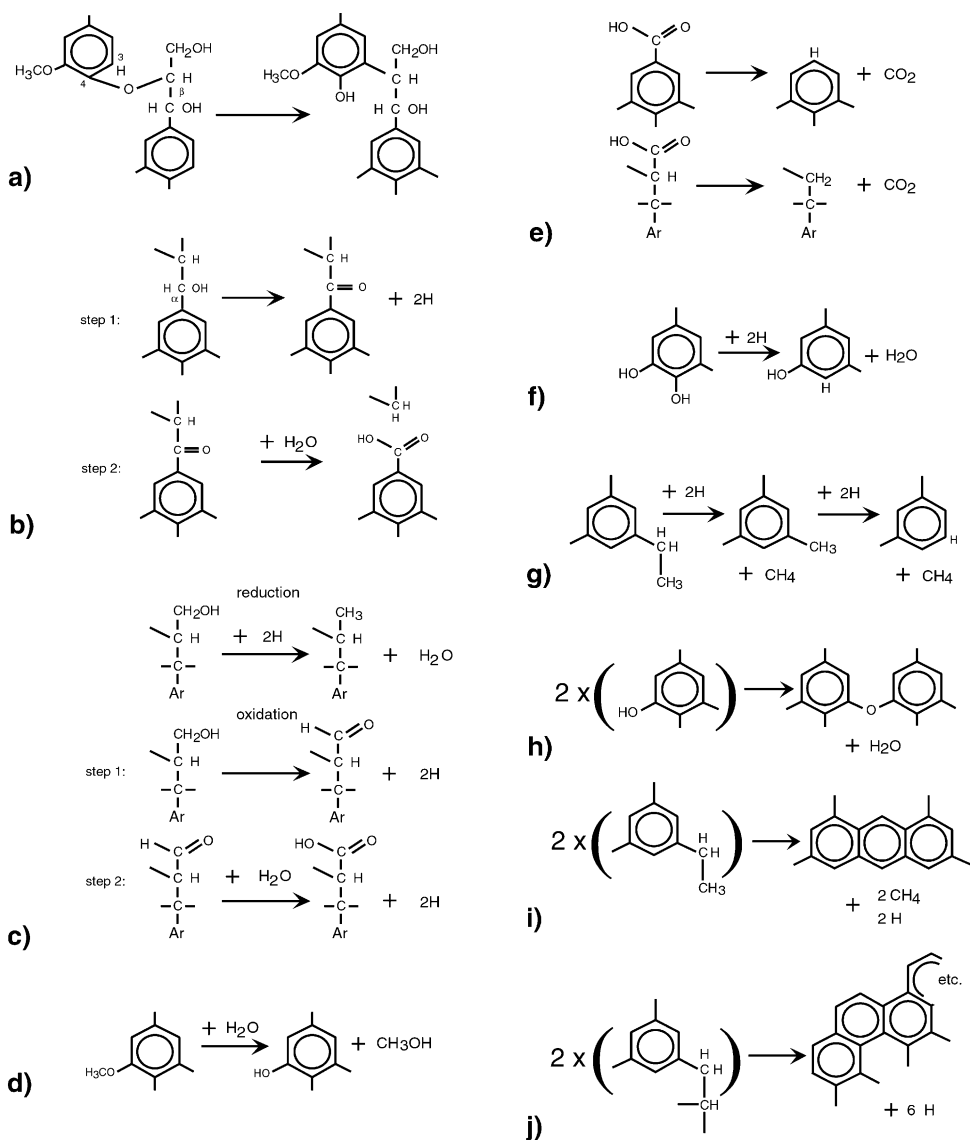
Fig. 2. Structural transformations of the lignin-derived macromolecule; (a) isomerization: cleavage of the β-O-4 linkage; this reaction results in no change in the elemental composition of the lignin; (b) progressive oxidation at the propyl α-site; this sequence is suggested by an increase in carbonyl groups with increasing thermal maturity up to the brown coal rank, followed by a decrease, and a concomitant increase in carboxyl functional groups; (c) transformation of the propyl γ-site from carboxyl to alcohol and methyl functional groups; this series illustrates hydrogen and water sources and sinks within the lignin structure; (d) transformation of an aromatic methoxyl to an aromatic hydroxyl functionality; this transformation is invoked by an inverse relationship between aromatic methoxyl and hydroxyl functional group content between unaltered lignin and sub-bituminous rank coal; (e) decarboxylation for both aromatic and aliphatic carboxyl groups is assumed to be a first order process; (f) dehydration of the aromatic structure is suggested to describe observed loss of aromatic hydroxyl functional groups between the lignite and sub-bituminous coal ranks; (g) progressive demethylation first from a pendant aryl-ethyl, and subsequently from a pendant aryl-methyl are suggested to account for methane generated primarily from aromatic functional groups; (h) cross-linking reaction associated with dehydration and formation of an aryl-ether linkage accounts for a relatively unchanged aromatic oxygen content associated with a total oxygen loss of about 50% by the high volatile bituminous coal rank; (i) cross-linking reaction associated with demethylation, which accounts for increasing condensation with thermal maturity; (j) cross-linking associated with loss of hydrogen, illustrating another means of condensation and creation of polyaromatic structures.

none is left by the sub-bituminous rank (Hatcher, 1990). Because there is little change in the quantity of aromatic oxygen substituents, the cleavage is believed to occur between the methyl and the oxygen, and the methyl group is replaced with a hydrogen atom to become an OH group (Fig. 2d). Although this reaction mechanism has not been approached from a geochemical standpoint, some experimental data on the reductive demethoxylation of simple methoxylated phenyls (anisoles) in the presence of strong reducing agents (alkali metals) show that in the presence of a hydrogen donor and an electron donor, demethoxylation occurs by cleavage of the methyl–oxygen bond, producing a phenol (Patel et al., 1982; Lazana et al., 1989; Azzena et al., 1996). Although such strong reducing agents are not found in the geochemical environment of lignin transformation, there are other reducing species available in the diagenetic system, most notably Fe and S species, or the organic species themselves. Given geological time scales, it is possible that such reductive reactions occur under natural coalification conditions. However, a suggested mobile product is methanol (P.G. Hatcher, personal communication), indicating that the reaction is not a reduction, but more likely an addition of water.

Decarboxylation is documented by a decreasing concentration of carboxyl functional groups with progressive maturation in the geologic environment after the lignite rank and through the high volatile bituminous rank (Hatcher, 1990; Hatcher et al., 1992), and by pyrolysis experiments as mentioned earlier. Thermal decarboxylation of simple aliphatic acids is observed to follow first-order rate laws (Kharaka et al., 1983). A suggested mechanism is by means of a catalyst, which causes cleavage between the aliphatic and carboxyl carbon atoms, and subsequent combination of the carboxyl proton and the aliphatic carbon (Bell and Palmer, 1994). However, in the case of the lignin-derived molecular structure, which is more complex and has more aromatic carboxyl functional groups, the mechanisms of decarboxylation may differ. In coal pyrolysis experiments, cross-linking of aromatic groups associated with decarboxylation suggests that the decarboxylation mechanism may indeed be a non-first order process (Suuberg et al., 1985; Solomon et al., 1990; Charpenay et al., 1996). However, in the model presented here, simple first-order decarboxylation reactions are assumed, occurring primarily at the propyl α-carbon and secondarily at the propyl γ-carbon where carboxyl functional groups are formed (Fig. 2e).

Loss of OH groups is likely to cause production of H_2O, and two elimination reactions may be responsible for the loss of hydroxyl substituent groups from the lignin-derived molecular structure. These dehydration reactions are inferred by NMR data which show a general reduction of oxygen functionalities with progressive coalification (Hatcher, 1990), and are further suggested by structural H_2O produced during pyrolysis (Behar and Hatcher, 1995). The OH groups may be lost from either of the hydroxylated alkyl sites (discussed above) or the aromatic sites (phenol groups are produced during β-O-4 cleavage and in the demethoxylation reaction; Fig. 2a and d). For maturities greater than the lignite rank and through the sub-bituminous rank, dehydration of aromatic sites is inferred from NMR evidence of the transformation of the aromatic structure from a catechol-like (two hydroxyl) to a phenol-like (one hydroxyl) structure (Hatcher, 1990). This is suggested to be the main cause of loss of oxygen from the lignin-derived molecular structure occurring at the sub-bituminous rank and later. In an environment with sufficient activated hydrogen, this transformation may occur as indicated in Fig. 2f. Loss of oxygen through cross-linking is discussed below.

It has been suggested that methane generated ranks higher than sub-bituminous and at higher pyrolysis temperatures are probably from functional groups attached directly to the aromatic structure (Behar and Hatcher, 1995; Charpenay et al., 1996). A variety of potential precursor alkyl functional groups have been observed on coals from lignite through low-volatile bituminous rank (Obeng and Stock, 1996). An increase in pyrolytic CH_4 generation rate with increasing rank (Charpenay et al., 1996) and an increase in pendant methyl groups (those attached directly to the aromatic structure) from unaltered lignin through the low volatile bituminous rank (Obeng and Stock, 1996) suggest that structural transformations which form the aromatic methyl functional groups are occurring simultaneously and more rapidly than demethylation, and that aryl methyl groups may not play an important role in methane generation until after the low-volatile bituminous rank. The model accounts for the presence of pendant alkyl groups through cleavage of the propyl chain by oxidation at the α-site. This results in the formation of a pendant ethyl group. The activation energy required to homolytically cleave an ethyl group from an aromatic ring is about 24 kcal/mol greater than that required to cleave a methyl from a pendant ethyl (Luo and Holmes, 1993). This reaction preference effectively increases the number of pendant methyl groups in the model. Thus, two methane-producing reactions incorporated in this model include demethylation of an aromatic pendant ethyl, and later demethylation of the resultant pendant methyl (Fig. 2g).

2.5. Class IV: cross-linking

During the coalification process the aromatic structures condense, or combine with each other, producing an increasingly graphitic molecular structure (Grant and Pugmire, 1989; Solum et al., 1989; Levine, 1993; Behar and Hatcher, 1995; Manion et al., 1996). This kind of reaction might occur when two carbon sites are made available for bonding, for example when a functional group has been removed. Pyrolysis experiments indicate that cross-linking may be associated with the generation

of CO_2, CH_4, and H_2O (Suuberg et al., 1985; Solomon et al., 1990; Hatcher et al., 1992; Charpenay et al., 1996). This model does not attempt to fully characterize the graphitization process, but it does incorporate cross-linking associated with dehydration, demethylation and loss of hydrogen. Cross-linking associated with decarboxylation is also discussed.

Cross-linking associated with loss of H_2O is observed in pyrolysis experiments (Solomon et al., 1990; Charpenay et al., 1996). Moreover, kerogen depeleted in oxygen-bearing functional groups during natural maturation is less likely to exhibit cross-linking in pyrolysis experiments (Burnham et al., 1989), suggesting that oxygen-bearing sites may be favorable for cross-linking processes. More importantly, studies of naturally matured lignin-derived molecular structures at the high volatile bituminous rank show that the aromatic-oxygen content has decreased little, but that total oxygen content has decreased by about 50% (Hatcher et al., 1992). This suggests that many of the remaining aromatic oxygen atoms are transformed into aromatic ethers, sharing one oxygen atom between two aromatic rings. A suggested reaction is represented in Fig. 2h.

Methane formation associated with cross-linking during pyrolysis experiments is observed at higher temperatures than cross-linking reactions associated with CO_2 or H_2O generation (Solomon et al., 1990). A suggested demethylation reaction involves cross-linking with loss of a methyl group from a pendant ethyl and recombination with an aromatic carbon to produce an anthracene-like structure (Fig. 2i). Additional methane may be generated during further condensation of anthracene- or naphthene-like structures, but this would require loss of carbons from the aryl-structures and probably significantly higher activation energies.

During the coalification process hydrogen is gradually lost relative to oxygen and carbon (Levine, 1993). This loss can be attributed to some of the processes described earlier, for example loss of hydroxyl functional groups, or demethylation. As the condensation continues, aromaticity increases, suggesting that carbon sites become increasingly unsaturated. Although this may occur due to loss of saturated carbons from aliphatic side chains and methoxyl groups, it is conceivable that cross-linking of aromatic structures with loss of hydrogen from saturated carbons may also occur (Fig. 2j). Although this reaction is speculative, it suggests another source of hydrogen atoms within the organic material, which allows hydrogen-consuming reactions to occur (for example demethylation of pendant methyl groups) (Fig. 2g).

3. Reaction network

3.1. Network construction

To construct the network, each structural transformation discussed above is formulated as a stoichiometrically balanced reaction. The reactant chemical species include the starting lignin-derived macromolecule (Fig. 1) and a suite of immobile intermediate species, which are defunctionalized or fragmented macromolecular parts of the starting macromolecular structure; the product species include residual immobile intermediate species, which serve as reactants in subsequent reactions, and mobile species, which may or may not be reactants in subsequent reactions. A given immobile species may be a product of one reaction and a reactant for another. The immobile species connect the reactions and form the framework of the reaction network. The mobile species are those smaller molecules that are released from the residual structure, and include CH_3OH, H_2O, CO_2, CH_4 and H* (an unspecified, reactive form of hydrogen). These are generally only reaction products, although H_2O and H* are reactants in some reactions.

The reactions are placed into a network under the following guidelines: (1) required sequence of reaction is preserved; for example, decarboxylation at the aromatic site (Fig. 2e) cannot proceed until after the reaction which forms that carboxyl group (Fig. 2b); and (2) competing, or parallel pathways are represented; for example oxidation versus reduction at the γ-OH site (Fig. 2c). The resulting network of sequential and parallel comprises 21 reactions involving 23 species (Fig. 3).
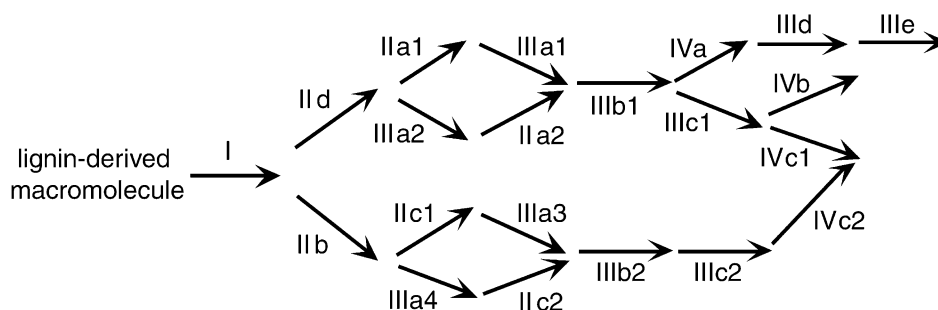
Fig. 3. The model reaction network comprises 25 species and 21 reactions, incorporating the 13 types of reactions listed in Table 1. Other reaction information is listed in Table 2.

3.2. Mathematical formulation

The chemical kinetic model representing this reaction network can be formulated using standard reaction-transport equations in the form of nth-order processes. The model focuses on the dynamics of the immobile macromolecular species, because these are the natural choice for calibration. As all reactions of these species are considered irreversible, the transformation of lignin-derived molecular structure is separable as follows. Let C_i be the moles of species i per rock volume and k_α^{eff} be an effective rate coefficient for the process α that consumes one or more i' reactant molecules and generates $v_{i\alpha}$ product molecules. Generation and consumption rates for all species can be described by

$$\frac{dC_i}{dt} = \sum_\alpha v_{i\alpha} k_\alpha^{\mathrm{eff}} \left(\prod_{i'} C_{i'(\alpha)} \right). \tag{1}$$

By convention, $v_{i\alpha}$ is -1 when i is being consumed by the α reaction, or $v_{i\alpha}$ is the number of i molecules produced by the α reaction. Because the reactions are nth order where n is an integer, the solution is strongly non-linear and must be solved iteratively. Computations are facilitated by using a time step that dynamically changes to minimize errors, to allow faster convergence, and to proceed with sufficient computational speed.

3.3. Calibration

Because the model is based on observed and inferred structural transformations, kinetics for the processes were derived not from laboratory derived pyrolysis experiments, but rather were estimated in such a way as to better capture the kinetics of the processes under geological conditions. Estimates of rates were made based on the timing of specific structural transformations relative to coal rank. For example, approximately 50% of the aromatic-methoxyl groups are lost between the unaltered lignin and brown coal stage (Hatcher, 1990); it can be roughly estimated that this occurs over a temperature range from 10 to 45 °C (Bouska, 1981). Solving the differential equation for rate

$$dc/dt = k \tag{2}$$

(c is concentration, t is time, k is the rate coefficient),

$$\ln c_0/c = kt \tag{3}$$

(c_0 is the initial concentration of reactant) the rate coefficient of demethoxylation (hence methanol production; Fig. 2d) can be estimated for this temperature range.

These processes are observed to be temperature dependent and thus, by convention, follow the Arrhenius law

$$k = A\exp(-E_{\mathrm{act}}/RT) \tag{4}$$

where k is the rate coefficient, A is the Arrhenius pre-exponential, E_{act} is the activation energy, R is the universal gas constant, and T is temperature. Because not enough information exists to solve for both A and E_{act} for geological reactions with available data, A is assumed to be constant for all reactions and is calculated independently from statistical mechanics:

$$A \cong KbT/h\exp(\Delta S_{\mathrm{act}}/R), \tag{5}$$

where Kb is Boltzman's constant, h is Planck's constant, and S_{act} is the activation entropy. Determining S_{act} requires knowledge of elementary mechanisms and transition state geometries of the molecules, which is beyond the scope of this model. Thus ΔS_{act} is assumed to equal zero, which is appropriate for first order reactions. When a constant is used for T (298 °C), A equals a constant value of 6.18×10^{12} s^{-1} for all reactions. From the estimated rate of each process, an estimated E_{act} is calculated from the Arrhenius law. Sensitivity testing indicates that changing values of A may shift the timing of the reaction, but does not significantly affect the shape of the reaction slope, unless it is changed by many orders of magnitude.

The estimated kinetic parameters were then refined and the model calibrated to the Piceance Basin. Upper Cretaceous Williams Fork Formation coals from the Piceance Basin are vitrinite-rich (approximately 90% vitrinite; Zhang et al., 1997) and, for the purpose of this model, are assumed to be derived largely from lignin. As a cautionary note, the authors acknowledge that there may be a contribution to these coals from some other non-lignin-derived macromolecule, which would possibly result in a significantly different reaction network and timing and abundance of evolved products than those presented here. Indeed, the samples comprise approximately 5% H-rich liptinite, a potentially significant precursor to methane, and the presence of which could affect the chemistry of the residual organic matter upon which the model is calibrated. More appropriate sample sets may be used for the calibration of the model, yet the approach would remain unchanged, and it is a simple first assumption to test this kind of kinetic structural modeling.

Using the estimated activation energies and an independently derived thermal and burial history (Comer et al., 1997), the model is run iteratively to calibrate the kinetics against observed C, H, and O weight percent of coal at the MWX Site. The calibration was constrained to preserve the relative sequence of observed structural transformations; for example, a reaction that sequentially follows another naturally should have a larger E_{act} value. Table 1 shows the activation energies determined for and used in the model. The calculated elemental

weight percents for the MWX coal were within the ranges of analytical values,

In order to assess the model, the predicted results were compared with observations for sixteen additional sites for which burial and thermal histories were independently determined (Lorenz, 1985; Johnson and Nuccio, 1986, 1993; Nuccio and Johnson, 1989). Because elemental weight percent values for C, H, and O are not available for these sites, but mean vitrinite reflectance (R_0) values are, the model uses calculated H/C and O/C ratios to calculate R_0 after the method of Burnham and Sweeney (1989). Fig. 4 compares the resulting R_0 values with observed values at each site [the Burnham and Sweeney (1989) method calculates a maximum R_0 value; however, the degree of anisotropy in the range of this model is not expected to significantly affect the relationship shown in this figure]. In general, the predicted and observed reflectance values differ by a maximum of 0.29% R_0, but most are within 0.2% R_0. The model generally predicts lower reflectance values at lower maturities, higher values at moderate maturities, and slightly lower values at the highest maturities over the range of observed maturities.

The resulting compositional change of the remnant immobile species is illustrated by the carbon, hydrogen, and oxygen elemental weight percents (Fig. 5). As expected, carbon content increases significantly over the course of the simulation, and oxygen decreases significantly. There is a net loss of hydrogen over the course of the simulation. Relative changes in atomic O/C and H/C ratios show the generally expected trend, similar to the trend for Type III kerogen (terrigenously-derived), with relative loss in O/C preceding relative loss of H/C (Fig. 6). Differences between model predicted and Type III atomic ratio trends may occur because the

model assumes a single molecular precursor, whereas Type III kerogen comprises multiple molecular precursors, and thus would have a chemistry representative of a composite of molecular precursors. The relative lack of change in the H/C ratio while O/C ratio values are decreasing additionally may be the result of the assumption of a closed system: all of the hydrogen that is generated from the reactions (as well as much of the H_2O) is assumed to be available as reactants for ensuing reactions. Hydrogen thus becomes incorporated back into the macromolecular structure, resulting in a higher H/C ratio than might be expected in an open system. At highest H/C and O/C values, the relationship between the ratios reflects earliest reactions in which there is a net loss of hydrogen relative to oxygen.

4. Discussion

As with any model there is uncertainty with underlying assumptions and values used for input and calibration parameters. Structural components of the macro-molecular structure that are omitted in this simplified model structure and the likelihood of other non-lignin-derived components in sedimentary organic matter from which coal is derived will undoubtedly affect the network of reactions that occur during maturation and hence the maturity indices, as well as the evolved product composition, timing and abundance. Important processes may occur during peatification that affect the structural characteristics of the starting material. Certainly, important processes occur beyond the degree of maturation to which this model is limited (about 1.7% R_0, or the low volatile bituminous rank) that affect the evolved product
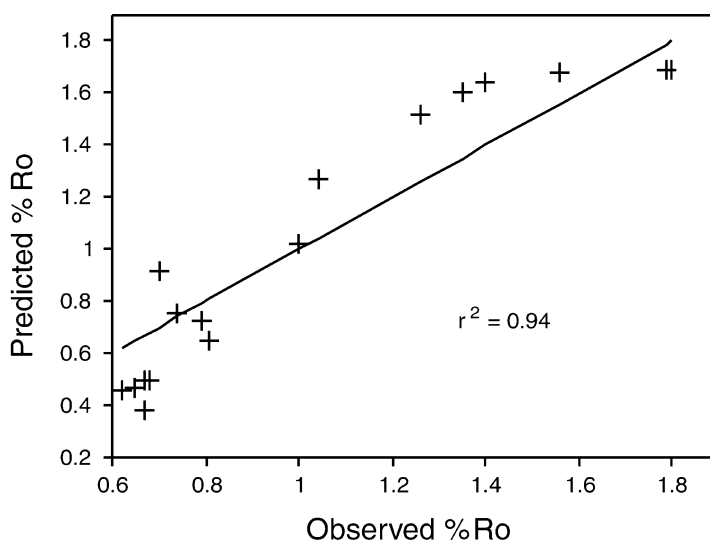
Fig. 4. Cross-plot of model calculated (after method of Burnham and Sweeney, 1989) and observed vitrinite reflectance values. Solid line has a slope of 1.0.
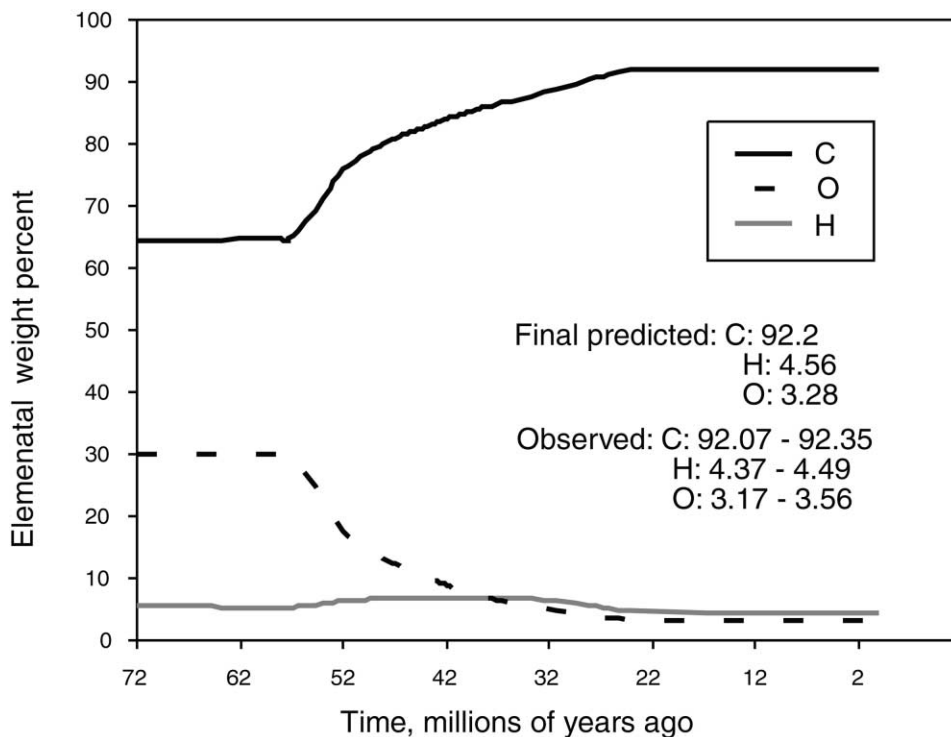
Fig. 5. Predicted residual chemistry through time at the MWX site: carbon, hydrogen, and oxygen elemental weight percents, with final predicted and observed values.
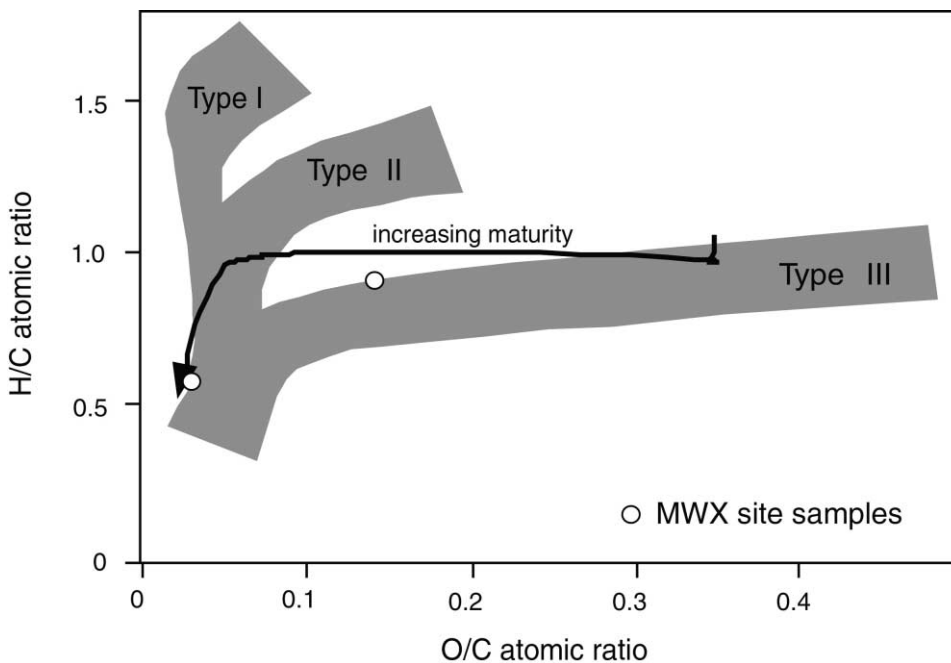
Fig. 6. H/C versus O/C atomic ratios of simulated residual sedimentary organic matter, shown with Type III kerogen trend, and MWX Site sample data.

generation. With increasing rank, however, characterizing the structural transformations analytically becomes increasingly difficult. Finally, any error in the input burial and thermal histories will also be embedded in the calculations of this model.

The essence of this model, and its novelty, are the identification of specific and characteristic molecular structures and linkages, and the reactions that transform them. This approach allows accounting for the natural variability and complexity of the lignin-derived macromolecule. The structure of the starting material is assumed in this model to be a simplified guaiacyl-like polymer when in reality, its form is more complex. For example, it is suggested that many of the propyl-α sites are occupied by hydroxyl functional groups, and that there may be some hydroxyl groups located on the aromatic structures. In addition, some ether linkages may connect propyl structures. The design of this model allows straightforward modification of the starting macromolecular composition to account for the statistical distribution of structures, linkages, and functional groups in order to account for greater complexity in the starting material. Specifically, the model may be modified to include several different types of monomers with different linkages. For example, if 50% of the linkages are of the β-O-4 type, 25% are of the α-O-4 type and 25% link propyl structures, then one would construct a model in which the starting material comprises 50, 25 and 25% of the molecules with these respective structures, each structural type having its own network of reaction pathways depending upon its initial structure. In the spirit of this modeling approach based on molecular structures, it would be assumed that most of the reaction stoichiometries and kinetics for a given reaction type would be the same. Many such modifications to the original macromolecular structure could be accounted for in this way, creating a larger and more complex reaction network, but allowing the fundamental processes and their kinetics to remain the same. With the increasing availability of better-constrained analytical data on molecular structures and transformations and reaction mechanisms, this kind of model can be calibrated more specifically and directly.

The model also includes the formalism to account for non-first order processes. Observations of certain structural changes indirectly suggest the occurrence of non-first order processes, for example reactions in which hydrogen or oxygen must be added to the structure, or cross-linking. Potential reactants, connate H_2O and hydrogen bound to the organic material itself, are probably sufficiently abundant. Naturally, if a reactant is scarce, reaction rates are slowed, and if abundant, rates increase. Direct evidence of the mechanisms involved is lacking, but the nth order reaction formalism allows more exact reactions to be modeled when or if specific evidence is available.

One of the unique features of this approach to modeling maturation is its versatility and potential applicability to various kerogen types in a variety of source rocks. Similarly designed models may be developed for a suite of selectively preserved proto-kerogen macromolecular species, each with its own reaction pathways, producing a unique set of intermediate and mobile species. Furthermore, such models may be combined to represent sedimentary organic matter derived from multiple sources. For example, a coal with a significant algal contribution might be represented by a model network comprising 75% lignin-derived macromolecule and 25% algaenan-derived macromolecule.

This type of model may be taken still further by considering that a specific depositional environment may be characterized by a distribution of resistant biomolecular components. One could distinguish a shallow marine carbonate source material from that of a delta by considering compositional differences in the amount of terrigenous versus marine biomolecular input. These are important factors that are expected to cause significant variations in timing and yields in gas-bearing versus oil-bearing petroleum systems, that are lost in models which are calibrated on standard kerogen types, or assume a single precursor composition with a highly generalized set of kinetic parameters. So, while the present treatment is limited to lignin-derived source material, this novel approach is not, but rather applies to the diverse classes of kerogen precursory molecules.

5. Summary

The model presented in this paper simulates the linin-derived molecular structural transformations that occur under natural geological conditions up to approximately low-volatile bituminous rank maturity. This model adopts a simplified guaiacyl polymer as the starting molecular structure, assuming that early microbial degradation has not significantly altered the lignin macromolecular structure. The transformations are described as individual reactions, which are placed in sequential order according to estimated thermal conditions during which each transformation occurs, and are constrained by the availability of reactant species. The structural transformations are described as 13 processes divided into four classes: isomerization, modification of the propyl structure, defunctionalization, and cross-linking. When the reaction network is established, kinetic parameters for each reaction are approximately assigned by an estimated thermal range for each transformation. The reaction network is then refined by calibrating the network specifically to elemental weight chemistry of Williams Fork coal from the MWX site in the Piceance Basin, CO, assuming that this coal is primarily lignin-derived. We would again caution that this assumption

does not consider the contribution of other biomacromo-lecular components to the SOM, which could, due to dif-fering chemistries, affect the resulting model calibration.

The novelty of this approach is that it utilizes what is known about the chemical structure and its natural transformations of a selectively preserved, major mole-cular component of sedimentary organic matter. This model accounts for compositionally specific reactants evolving to compositionally specific products rather than empirical fitting of bulk chemistry. This type of model can also be applied to other major molecular components of kerogen, such as algaenan or cutan. Because some of the structural components of the spe-cies are the same, the kinetic behavior of some reactions would be expected to be similar. Such models could be used to model the transformation of a composite mix-ture of starting materials, as one might expect to find in most sedimentary environments. Furthermore, as this model accounts for stoichiometric product generation, the model can use volumetric estimates of starting mole-cular species to calculate the molar amount of products generated such as methane. This kind of application is explored in Part II of this contribution.

References

Azzena, U., Denurra, T., Melloni, G., 1996. Electron-transfer-induced reductive dealkoxylation of alkyl aryl ethers. II. Reductive cleavage of isomeric dimethoxybenzenes. Gazzetta Chimica Italiana 126, 141–145.

Behar, F., Hatcher, P.G., 1995. Artificial coalification of a fos-sil wood from brown coal by confined system pyrolysis. Energy and Fuels 9, 984–994.

Bell, J.L.S., Palmer, D.A., 1994. Experimental studies of organic acid decomposition. In: Pittman, E.D., Lewan, M.D. (Eds.), Organic Acids in Geological Processes. Springer Ver-lag, Berlin, pp. 226–269.

Bouska, V., 1981. Geochemistry of Coal. Elsevier Scientific, New York.

Britt, P.F., Buchanan III, A.C., Thomas, K.B., Lee, S.-K., 1995. Pyrolysis mechanisms of lignin: surface-immobilized model compound investigation of acid-catalyzed and free-radical reaction pathways. Journal of Analytical and Applied Pyrolysis 33, 1–19.

Buchanan III, A.C., Britt, P.F., Struss, J.A., 1997. Investiga-tion of reaction pathways involved in lignin maturation. Energy and Fuels 11, 247–248.

Burnham, A.K., Oh, M.S., Crawford, R.W., 1989. Pyrolysis of argonne premium coals: activation energy distributions and related chemistry. Energy and Fuels 3, 42–45.

Burnham, A.K, Sweeney, J.J., 1989. A chemical kinetic model of vitrinite maturation and reflectance. Geochimicia et Cos-mochimica Acta 53, 2649–2657.

Charpenay, S., Serio, M.A., Bassilakis, R., Solomon, P.R., 1996. Influence of maturation on the pyrolysis products from coals and kerogens. 2. Modeling. Energy and Fuels 10, 26–38.

Comer, J.B., Payne, D.F., Sibo, W. 1997. Modeling Burial and Thermal History of the Mesaverde Group, Piceance Basin, Colorado—Implications for Gas Generation from Coals. Abstract, AAPG Annual Meeting, Dallas, p. A22.

del Rio, J.C., Gonzalez-Vila, F.J., Martin, F., Verdejo, T., 1994. Characterization of humic acids from low-rank coals by ^{13}C-NMR and pyrolysis-methylation; formation of ben-zenecarboxyl acid moieties during the coalification process. Organic Geochemistry 22, 885–891.

Gilbert, K.E., Gajewski, J.J., 1982. Coal liquefaction model studies: free radical chain decomposition of diphenylpro-pane, dibenzyl ether, and phenyl ether via β-scission reac-tions. Journal of Organic Chemistry 47, 4899–4902.

Grant, D.M., Pugmire, R.J., 1989. Chemical model of coal devolatilization using percolation lattice statistics. Energy and Fuels 3, 175–186.

Hartgers, W.A., Sinninghe Damste, J.S., deLeeuw, J.W., 1995. Curie-point pyrolysis of sodium salts of functionalized fatty acids. Journal of Analytical and Applied Pyrolysis 34, 191–217.

Hatcher P.G., 1990. Chemical structural models for coalified wood (vitrinite) in low rank coal. In: Durand, B. Behar, F. (Eds.), Advances in Organic Geochemistry 1989, Pergamon, Oxford. Organic Geochemistry, 16, 959–968.

Hatcher, P.G., Faulon, J.-L., Wenzel, K.A., Cody, G.D., 1992. A structural model for lignin-derived vitrinite from high-volatile bituminous coal (coalified wood). Energy and Fuels 6, 813–820.

Johnson, R.C., Nuccio, V.F., 1986. Structural and thermal history of the Piceance Creek Basin, Western Colorado, in relation to hydrocarbon occurrence in the Mesaverde Group. In: Spencer, C.W., Mast, R.F. (Eds.), Geology of Tight Gas Reservoirs. AAPG Studies in Geology, vol. 24, pp. 165–205.

Johnson, R.C., Nuccio, V.F., 1993. Surface Vitrinite Reflec-tance Study of the Uinta and Piceance Basins and Adjacent Areas, Eastern Utah and Western Colorado—Implications for the Development of Laramide Basins and Uplifts. US Geological Survey Bulletin 1787-DD, p. 38.

Kharaka, Y.K., Carothers, W.W., Rosenbauer, R.J., 1983. Thermal decarboxylation of acetic acid: implications for ori-gin of natural gas. Geochimica et Cosmochimica Acta 47, 397–402.

Kuroda, K.-I., 1995. Contribution of an oxirane intermediate in the pyrolytic cleavage of the β-aryl ether substructure in lignin: pyrolysis of 3,4-dimethoxyphenyloxirane. Journal of Analytical and Applied Pyrolysis 35, 53–60.

Lazana, M.C.R.L.R., Franco, M.L.T.M.B., Herold, B.J., 1989. Electron-spin distribution in radical anions of aryl methyl ethers vs. reactivity and regioselectivity of their unimolecular fragmentation. Journal of the American Chemical Society 111, 8640–8646.

Levine J.R., 1993. Coalification: the evolution of coal as source rock and reservoir rock for oil and gas. In: Law, B.E., Rice, D.D. (Eds.), Hydrocarbons from Coal. AAPG Studies in Geology, Vol. 38, pp. 39–77.

Lorenz, J.C., 1985. Tectonic and Stress Histories of the Piceance Creek Basin and the MWX Site, from 75 m.y.a. to present. Sandia National Laboratories report SAND84-2603, UC-92.

Luo, Y.-R., Holmes, J.L., 1993. The prediction of bond dissociation energies for common organic compounds. Journal of Molecular Structure 281, 123–129.

Manion, J.A., McMillen, D.F., Malhotra, R., 1996. Decarboxylation and coupling reactions of aromatic acids under coal-liquefaction conditions. Energy and Fuels 10, 776–788.

Michels, R., Langlois, E., Ruau, O., Mansuy, L., Elie, M., Landais, P., 1996. Evolution of Asphaltenes during artificial maturation: a record of the chemical processes. Energy and Fuels 10, 39–48.

Nuccio, V.F., Johnson, R.C., 1989. Variations in vitrinite reflectance values for the Upper Cretaceous Mesaverde Formation, southeastern Piceance Basin, northwestern Colorado—implications for burial history and potential hydrocarbon generation. US Geological Survey Bulletin 1787-H.

Obeng, M., Stock, L.M., 1996. Distribution of pendant alkyl groups in the Argonne premium coals. Energy and Fuels 10, 988–995.

Patel, K.M., Baltisberger, R.J., Stenberg, V.I., Woolsey, N.F., 1982. Reductive cleavage mechanism of diphenyl ether and apparent ipso trapping of an intermediate radical anion with a silyl ether. Journal of Organic Chemistry 47, 4250–4254.

Petit, J.C., 1991. A comprehensive study of the water vapour/coal system: application to the role of water in the weathering of coal. Fuel 70, 1051–1058.

Solomon, P.R., Serio, M.A., Carangelo, R.M., Bassilakis, R., Gravel, D., Baillargeon, M., Baudais, F., Vail, G., 1990. Analysis of the Argonne premium coal samples by thermogravimetric fourier transform infrared spectroscopy. Energy and Fuels 4, 319–333.

Solum, M.S., Pugmire, R.J., Grant, D.M., 1989. ^{13}C Solid-state NMR of Argonne premium coals. Energy and Fuels 3, 187–193.

Song, C., Saini, A.K., Schobert, H.H., 1994. Effects of drying and oxidation of Wyodak subbituminous coal on its thermal and catalytic liquefaction. Spectroscopic characterization and products distribution. Energy and Fuels 8, 301–312.

Stalker, L., Farrimond, P., Larter, S.R., 1994. Water as an oxygen source for the production of oxygenated compounds (including CO_2 precursors) during kerogen maturation. In: Telnaes, N. van Graas, G. Øygard, K. (Eds.), Advances in Organic Geochemistry 1993, Pergamon, Oxford. Organic Geochemistry, 22, 477-486.

Suuberg, E.M., Lee, D., Larsen, J.W., 1985. Temperature dependence of crosslinking processes in pyrolysing coals. Fuel 64, 1668–1671.

Tegelaar, E.W., deLeeuw, J.W., Derenne, S., Largeau, C., 1989. A reappraisal of kerogen formation. Geochimica et Cosmochimica Acta 53, 3103–3106.

Zhang, E., Tang, Y., Hill, R., Liu, J., Foss, D.C., Chung, E.Y., 1997. Kinetic and Basin Modeling of Gas Generation form the Cameo Coal, Piceance Basin, Northwest Colorado. Chevron internal report.